AD-A102 321 ELECTRONICS RESEARCH LAB ADELAIDE (AUSTRALIA) F/G 20/7
A UNIVERSAL SOLID ION SOURCE.(U)
OCT 80 J RICHARDS
UNCLASSIFIED ERL-0175-TR NL

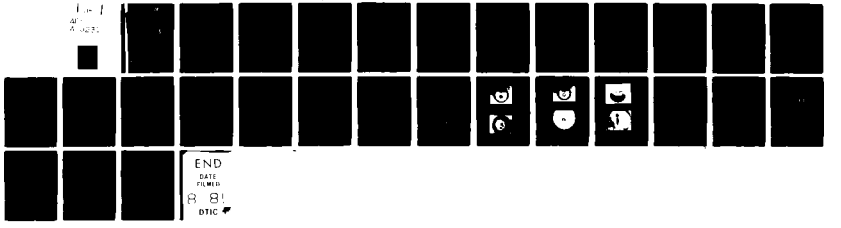

END
DATE FILMED
8 81
DTIC

ERL-0175-TR

AR-002-060

LEVEL II

12

DEPARTMENT OF DEFENCE

DEFENCE SCIENCE AND TECHNOLOGY ORGANISATION

ELECTRONICS RESEARCH LABORATORY

DEFENCE RESEARCH CENTRE SALISBURY
SOUTH AUSTRALIA

TECHNICAL REPORT
ERL-0175-TR

A UNIVERSAL SOLID ION SOURCE

J. RICHARDS

Approved for Public Release

OCTOBER 1980

AR-002-060

DEPARTMENT OF DEFENCE

DEFENCE SCIENCE AND TECHNOLOGY ORGANISATION

ELECTRONICS RESEARCH LABORATORY

TECHNICAL REPORT

ERL-0175-TR

A UNIVERSAL SOLID ION SOURCE

J. Richards, PhD.

SUMMARY

An ion source capable of generating ions from a wide range of normally solid materials is described. The source operates by focussing a powerful electron beam onto a molten target, the electrons serving to both vapourise and ionise atoms of the target. The ion beam drawn from the source possesses many desirable properties including a low energy spread, very high purity and high brightness.

POSTAL ADDRESS: Chief Superintendent, Electronics Research Laboratory, Box 2151, GPO, Adelaide, South Australia, 5001.

DOCUMENT CONTROL DATA SHEET

Security classification of this page: UNCLASSIFIED

1 DOCUMENT NUMBERS

AR Number: AR-002-060

Report Number: ERL-0175-TR

Other Numbers:

2 SECURITY CLASSIFICATION

a. Complete Document: Unclassified

b. Title in Isolation: Unclassified

c. Summary in Isolation: Unclassified

3 TITLE

A UNIVERSAL SOLID ION SOURCE

4 PERSONAL AUTHOR(S):

J. Richards

5 DOCUMENT DATE:

October 1980

6 6.1 TOTAL NUMBER OF PAGES: 13

6.2 NUMBER OF REFERENCES: 18

7 7.1 CORPORATE AUTHOR(S):

Electronics Research Laboratory

7.2 DOCUMENT SERIES AND NUMBER

Electronics Research Laboratory 0175-TR

8 REFERENCE NUMBERS

a. Task: DST 79/177

b. Sponsoring Agency: RD 73

9 COST CODE:

313330

10 IMPRINT (Publishing organisation)

Defence Research Centre Salisbury

11 COMPUTER PROGRAM(S) (Title(s) and language(s))

12 RELEASE LIMITATIONS (of the document):

Approved for Public Release

12.0	OVERSEAS	NO		P.R.	1	A		B		C		D		E	

Security classification of this page: UNCLASSIFIED

Security classification of this page: UNCLASSIFIED

13 ANNOUNCEMENT LIMITATIONS (of the information on these pages):

No limitation

14 DESCRIPTORS:

a. EJC Thesaurus Terms: Ion sources; Electron beams; Irradiation; Liquids; Solids

b. Non-Thesaurus Terms:

15 COSATI CODES:

2008

16 LIBRARY LOCATION CODES (for libraries listed in the distribution):

17 SUMMARY OR ABSTRACT:
(if this is security classified, the announcement of this report will be similarly classified)

An ion source capable of generating ions from a wide range of normally solid materials is described. The source operates by focussing a powerful electron beam onto a molten target, the electrons serving to both vapourise and ionise atoms of the target. The ion beam drawn from the source possesses many desirable properties including a low energy spread, very high purity and high brightness.

Security classification of this page: UNCLASSIFIED

TABLE OF CONTENTS

LIST OF TABLES

LIST OF FIGURES

1. INTRODUCTION

In a study of the effects of ion irradiation on the growth of thin films(ref.1) a need arose for an ion source capable of generating ions of materials normally solid at room temperature. Other requirements for the source included high purity, low energy spread, low gas load, medium current capability (tens of microamps) and the ability to form the ions into a beam. A study of the available types of solid ion sources led to the investigation of a type of source first used by Krimmel(ref.2,3,4) and investigated by other workers(ref.5,6,7). In this source, ions are generated when a powerful electron beam is focussed onto a solid target. This report describes a source based on Krimmel's work in which several modifications have been made in order to meet all of our requirements.

2. ION SOURCE DESIGN

A diagram of the ion source is shown in figure 1. An electron beam is generated in a telefocus electron gun(ref.4) and is focussed onto the target by an electrostatic einzel lens. At a typical electron energy of 30 k eV and a current of 3 mA the spot size is about 0.2 mm across, giving a power density of 2.9×10^5 W/cm^2 at the target. This power density is sufficient to form a hot spot in the target at which ions and vapour are generated.

In Krimmel's source the target is apparently solid, however, we found that for solid targets, stable emission would not occur. In such cases, it was observed that after a few seconds of operation a hole developed in the solid surface as material evaporated away from the hot spot. As this hole grew two effects occurred that altered the dependence between the ion current generated and the incident electron beam power. One was that the temperature of the hot spot fell, requiring an increasing electron beam power to maintain temperature. The other was that ions found it more difficult to escape, probably due to electrostatic screening effects. The elimination of such a hole is only assured if the target can flow, that is, it must be in the liquid state. With liquid targets stable ion emission always occurred. For targets having a melting point below about 500^{0}C, eg tin, it was a simple matter to construct a crucible with sufficiently low thermal losses that the 90 W of incident electron beam power was able to maintain the target in the molten state. For higher melting point materials, eg germanium, it was found necessary to heat the crucible independently with a resistive element.

The extraction of ions into a beam was performed by the electrode geometry shown in figure 1. In generating the beam use was made of the process known as plasma boundary focussing(ref.8), in which the plasma generated in the hot spot was allowed to expand above the target under the influence of the electric field of the extractor electrode. In order that a cylindrically symmetric ion beam be generated, the electric field in the region of the plasma must also be cylindrically symmetric, and this was approximately achieved by using the concentric conical electrodes shown in figure 1.

The ion beam, after passing through the extractor, was focussed by an electrostatic einzel lens into an approximately parallel beam about 2 mm in diameter. This beam was then directed into a 45^0 electrostatic deflector which bends the beam into a horizontal direction and also separates the ions from the vapour that is generated in the source.

Energy analysis of the ions generated in the source was performed with a high resolution parallel plate electrostatic analyser(ref.9) that was placed in the position normally occupied by the 45^0 electrostatic deflector. Mass analysis of the ion beam was obtained using a 45^0 magnetic sector analyser situated in the horizontal beam line about 2 m away from the source. Detection of ions

after passing through the mass analyser was achieved using a sensitive scintillation detector(ref.10).

3. PERFORMANCE OF SOURCE

The shape of the ion beam in the plane of the extractor is shown in figure 2. This result was obtained by placing a copper disc in the extractor and allowing ions and vapour to strike it. Tin was used in this experiment, the ion energy being 10 kV, the ion current 20 μA and the duration of the experiment 300 s. Just below the centre of the disc is an elliptical region about 0.3 mm by 0.4 mm in size where the ion flux is sufficiently intense for the sputtering rate to exceed the deposition rate of tin vapour, and the copper is exposed.

As can be seen in figure 3, the centre of this region has a depression about 65 μm deep and 60 μm across that is caused by an intense core containing about 5% of the total ions. The area of the beam defined by the region of exposed copper contains about half the total ions. Beyond this region, the ion flux is insufficient to remove all the depositing tin, hence a tin film develops. However, its appearance does vary because there is a strong dependence between the surface structure of tin films and the ratio of the ion to vapour flux during growth(ref.1). The light appearance is caused by high ion to vapour flux ratios (greater than 5%) the dark appearance by low ion to vapour flux ratios (between 1% and 0.1%) and the intermediate appearance by negligible ion to vapour flux ratios (less than about 0.05%). Thus figure 2 reveals that the beam profile is axially symmetric and drops off reasonably steadily with increasing distance from the beam core. There is a slight increase in ion density at large distances from the beam centre as evidenced by the annular dark region near the edge of the disc.

To examine the ion trajectories in the central part of the beam we performed an experiment in which a 0.7 mm diameter hole was drilled into the extractor on the beam axis and a further disc was placed some 7 mm beyond it, with the space between effectively field free. The results of this experiment are shown in figure 4, and they reveal that the beam passing through the extractor is divergent with a half angle of about 9^0. The uniformity of the beam appears reasonably good and it is quite cylindrical. These attributes make it reasonably easy to form the ions into a beam capable of travelling quite large distances.

Data derived from experiments like these enable a lower limit to be placed on the brightness of the ion beam generated in the source. It is best to evaluate the normalised brightness because it allows comparison with other sources. This is defined by the expression(ref.11)

$$B = \frac{9.4 \times 10^8 . A . I}{\Phi . \alpha^2}$$

where A is the ion mass in amu, I is the beam current in milliamps, Φ is the beam energy in volts and α is the beam emittance. Assuming the highest possible beam emittance consistent with the beam limits defined by the extractor aperture and by the beam shape etched on the plate behind the extractor, the brightness is 2×10^9, a value that compares quite favourably with that of many gas ion sources(ref.8).

It is interesting to compare the photographs shown in figures 3 and 4 with the result obtained when the extractor geometry consists simply of a biassed disc held above the surface of the target, ie the geometry used by Krimmel(ref.2).

As can be seen in figure 5 the beam is now crescent shaped and far from being axially symmetric.

The ion trajectories in this case were similarly investigated by drilling a hole in the extractor at the position shown in figure 5 and placing a plate some 12 mm beyond it. As can be seen in figure 5 the ions striking the crescent possessed a wide range of directions, are not uniformly distributed and are also not axially symmetric. These properties make it very difficult to direct ions generated with this extractor geometry into a beam.

4. OPERATION WITH DIFFERENT MATERIALS

The need to operate the source with the target in the liquid phase places a limitation on which elements the source can efficiently handle. This limitation comes about because it is undesirable to have too much material loss through evaporation from the liquid surface of the target. If we require that the lifetime of one crucible charge be at least 30 min then only those materials with a vapour pressure below about 0.1 torr at the melting point are suitable. The following normally solid elements are therefore unsuitable for use in the source in its present configuration; Mg, P, Ca, Cr, Mn, Zn, Sr, Cd, Sb, Te, Ba, Sm, Eu and Yb. Further, the very high melting point elements, eg C, W, Re may be difficult to use because of problems in maintaining them in a liquid state. However, ions of all other elements should be efficiently generated.

Ions of elements excluded on vapour pressure grounds could be generated if a shorter crucible lifetime were acceptable. Alternatively, it should be possible to redesign the source region in such a way that evaporation losses are considerably reduced eg by using a partially enclosed crucible. However, we made no attempt to do this as the source readily generated the ions of interest to us.

The source has been tested with Sn, Ge, In and Ag. With the exception of Ge the samples were held in a tantalum crucible maintained at a temperature above the melting point since this ensured they were molten. In the case of germanium two difficulties curred when the crucible was held above the melting point, one was that the germanium flowed out of the crucible when wetting occurred and the other was that the germanium chemically attacked the crucible. These problems were eliminated by keeping the temperature of the crucible about 200^{0}C below the melting point, in which case wetting does not occur. The germanium however could be easily held above the melting point by using the power of the electron beam and relying on the poor thermal contact between crucible and germanium. This technique is probably suitable for most materials that are reactive at high temperatures eg silicon, although of course we have only proved the method for germanium.

5. ION CURRENT

The dependence of ion current passing through a 1 mm diameter hole in the extractor on the electron beam current is shown in figure 6. The results are for tin and germanium ion beams and indicate that currents up to 20 μA for tin and 12 μA for germanium can be generated at energies up to 7.5 KeV. Since all the ions passing through the small hole in the extractor can be directed into a beam, these currents equal the currents that can be directed into the horizontal beam line. The maximum current so far obtained from the source is over 300 μA of tin ions using an extractor geometry consisting of an unshielded extractor held at 10 kV placed about 12 mm from the hot spot ie similar to the system used by Krimmel(ref.2). The reduced current obtained using the geometry of figure 1 is presumably caused by the

electrostatic screening effects of the conical electrode maintained at crucible potential.

In order to generate higher ion currents, it is likely(ref.8) that higher extraction energies, a reduced extractor-target separation and a more powerful electron beam would all improve the source's performance but it is not possible at this stage to state its upper limit.

6. BEAM ENERGY SPREAD

A typical energy spectrum of a tin ion beam obtained using a parallel plate analyser is shown in figure 7. The width of the spectrum is quite small, having a full width half maximum (FWHM) value of only 0.7 eV. However, most of this spreading is caused by the finite resolution of the analyser. At the ion energy used, 200 eV, a resolution of 1 in 500 gives an uncertainty of 0.4 eV in the energy analysis, indicating that the FWHM energy spread of the ions is about 0.3 eV.

7. BEAM PURITY

The results of the mass analysis of tin and germanium ion beams are shown in figures 8, 9 and 10 and also in Tables 1 and 2. The yields of the various peaks depended somewhat on source conditions in a complex manner, hence the values given are subject to quite large variations. Also, no correction has been made to the yields to allow for the dependence of detector sensitivity on ion species. Bearing in mind these limitations, the yields of many of the peaks are probably uncertain by a factor of 5 or so.

The tin results, as Table 1 shows, indicates the presence of 31 different ion species with a yield exceeding 0.001%, the limit of detectability. The number of lines in the mass spectrum, however, far exceed this number due to the many isotopes present. Of the 31 species, 19 are of tin in different charge states. The presence of tin in these cases was confirmed by the presence of a group of peaks containing the characteristic isotopic 'fingerprint' of tin. Most of these tin peaks can be readily identified as either multiply ionised tin or singly ionised tin clusters. The Sn^{120} peaks at m/e values of 150, 90, 66.7, 53.3, 45, 37.5, 33.6 and 28.8 however, cannot be related to any simple charge state. The origin of these peaks is discussed later.

The remaining peaks in the mass spectrum have been traced to two sources. The following ions, namely H_2O^+, OH^+, H_2^+, N_2^+, N^+, O_2^+, O^+ arise from ionization of the residual gases in the vacuum system. This conclusion was drawn from the observation that these peaks were always present irrespective of the power of the electron beam. Thus these ions are produced whether or not a hot spot is formed. This suggests that the ions do not come from the target and the only other possibility is that they are formed by ionization of background gases.

The other source of "non-tin" peaks has been traced to impurities present in the target, which is stated to be 99.96% pure tin. The yield of the copper, bismuth and lead peaks considerably exceeds the expected levels of these elements, since the sample used had these impurities at stated levels of 0.0025%, 0.002%, and 0.01% respectively. Another result observed is that the yield of these impurity ions steadily decreased with time such that after about 1 hour of continuous operation the lead and bismuth peaks fell below the limit of detectability whilst the copper peaks were just barely detectable. The results in Table 2 were obtained within the first 15 min of use of a freshly filled crucible.

Other impurities stated to be present in the tin were iron, arsenic and antimony. Any iron and antimony peaks would fall on or close to large peaks caused by tin hence it is not possible to detect them. In the case of arsenic, it has such a high vapour pressure at the temperature of the crucible (33 torr at 500^{0}C), that it is likely it will all evaporate before a measurement can be made.

The germanium results are similar in many ways to those for tin. There are multiply ionized species and singly ionised clusters. Further there is a germanium peak at 55.5, the origin of which is probably the same as the origin of the 90 peak in the tin spectrum, since both occur at m/e values of exactly 3/4 of the parent isotope.

There are also water vapour, nitrogen and oxygen peaks presumably caused again by ionization of background gases. The principal difference between the tin and germanium results is that no impurity ions of normally solid materials were present in the case of germanium. This result is expected in view of the fact that the stated purity of the germanium is 99.999%, indicating that any impurities would be too small to detect.

Several interesting conclusions can be drawn from the mass spectrum results.

(1) The lack of tantalum ions in the ion beams indicate that the crucible does not introduce any impurities into the beam.

(2) The purity of the ion beam is mainly governed by the purity of the starting material and this can be very high. The only impurities that are intrinsic in the source are those caused by ionization of the background gases and amount to about 0.1%. One method of reducing them is to use a better vacuum - there should be a roughly linear dependence between the yield of background gas ions and pressure. Another possible method of reducing the level of these ions is to maintain the potential of the regions where they are generated at a different level to the potential of the crucible. If this is done, these ions, on extraction, would possess a different energy and would therefore be efficiently separated from the desired species by the 45^{0} electrostatic deflector. This technique has not been proven because it was impossible in our apparatus to electrically isolate the crucible from the main body of the source. However, we feel such a technique should be capable of reducing the level of background ions in the horizontal beam line considerably.

The only outstanding problem associated with the mass spectra is the origin of the tin peaks at m/e values of 150, 90, 66.7, 53.3, 45, 37.5, 33.6 and 28.8 and the origin of the germanium peak at 55.5. All these peaks can be explained by charge exchange reactions as the ions pass along the horizontal beam line. These reactions would have to occur after passing through the 45^{0} electrostatic deflector because otherwise the reaction products would not be directed into the horizontal beam line. Table 3 gives a list of possible charge exchange reactions and the position on the mass scale at which the reaction product is located assuming that no energy is lost during the reaction. This assumption is justified because electron exchange reactions involve energies of several electron volts at most, which are negligible compared to the several thousand electron volts that the ions possess. One can see from Table 3 that all the peaks mentioned above can be explained. Further, the yields of most of the peaks are as expected assuming that the yield is (a) proportional to the yield of the precursor ion and (b) inversely proportional to the change in charge state that occurs during the reaction. The only exceptions are that the reaction $Sn^{7+} \rightarrow Sn^{5+}$ appears more likely than $Sn^{7+} \rightarrow Sn^{6+}$ and the reaction $Sn^{6+} \rightarrow Sn^{4+}$ is more likely than $Sn^{6+} \rightarrow Sn^{5+}$. The stability of these highly ionised species is probably a complex function

of many parameters, hence these two slight discrepancies do not, we feel, disprove our model of their origin.

The precise mechanism whereby the charge exchange reaction takes place has not been determined. Two mechanisms are possible, one is through a charge exchange collision with a residual gas molecule in the beam line and the other is the acquisition of a free electron. Such electrons could be generated, for example, by ion impact with the walls of the beam line. We have been unable to find published data for charge exchange reactions of highly ionised tin or germanium ions, hence an assessment of the likelihood of each mechanism is difficult to make.

The peaks associated with charge exchange reactions have, to our knowledge, not been observed previously. There are perhaps two reasons for their detection in our case. The first is that our detector is sensitive to ions over a wide energy range, whereas the type of detector usually employed in such studies looses sensitivity if the energy to charge ratio of the ions differs from an ideal value by more than about 20%(ref.12). In the majority of cases, charge exchange reactions cause the energy to charge ratio to move beyond this 20% limit and thus beyond the ability of the detector to respond. The other reason is that the length of our beam line along which the ions travel (2 m) is probably longer than is common, hence charge exchange reactions are more likely.

8. IONIZATION MECHANISM

Schwarz(ref.13) has postulated that during the interaction of a high power electron beam with a target, a plasma column is formed beneath the surface of the target. The existence of this column inside the target was verified in our case by using a target that was able to cool very rapidly, in less than half a second. In this case, when the electron beam was suddenly switched off a hole about 0.2 mm across and 1 mm deep was left in the centre of the solidified target where the electron beam had been focussed. Presumably this hole is that previously occupied by the plasma. In this section we describe the results of experiments designed to evaluate the temperature and pressure of the plasma and the mechanism producing ionization.

Using tin as the working material, and an unshielded extractor, it was found that the ion generation rate was proportional to the evaporation rate from the target with a constant of proportionality of 0.07% ± 0.02%. At an ion current of 120 μA, a typical value, the corresponding evaporation rate was 2.28×10^{-4} g/s. If we assume that the majority of the material lost from the target emerges from the spot struck by the electron beam, then the evaporation rate is 0.726 g cm^{-2} s^{-1} from the 0.2 mm diameter emitting region. Langmuir(ref.14) has shown that the evaporation rate of most metals in vacuum is given by

$$R = 5.85 \times 10^{-5} P \sqrt{\frac{M}{T}} \text{ g . cm}^{-2} \text{ . s}^{-1}.$$

where P is the vapour pressure in microns of mercury, T is the temperature in ^{0}K and M the molecular weight of the metal. Using this expression and published data for the vapour pressure of tin as a function of temperature(ref.15) we find that the temperature of the hot spot is $2440^{0}K$ and that the vapour pressure of tin in the plasma column is 68 torr.

Bearing in mind these parameters, we feel that the most likely mechanism causing ionization is a collision between the incident electrons and the metal

vapour present in the column. An estimate of the ionization rate by this mechanism is difficult because published ionization cross sections for electrons passing through tin vapour are not available. However, as a rough approximation we can use the ionization efficiency of mercury vapour(ref.16) which, for electrons at an energy of 30 kV, is about 0.2 ion pairs/cm, per millimetre mercury per electron at 0^{0}C. At 2440^{0}K and 68 torr, the ionization rate would be 1.5 ions/cm for each incident electron. Assuming a column length of 1 mm, the ionization rate becomes 0.15 ions/electron which, for a 3 mA electron beam, gives an ion generation rate of 450 μA. The observed current, 120 μA, could therefore be readily accounted for by this ionisation mechanism.

The presence of highly ionized species in the ion beam is a feature that confirms non-equilibrium phenomena are responsible for producing ionization in the plasma. For example, if thermal ionization was responsible for generating the ions, the yield of doubly ionized tin would be 10^{15} times smaller than the yield of singly ionized tin, far smaller than the observed yield, which is only four times lower than that of Sn^{+}.

9. CONCLUSION

The design and operation of an ion source capable of generating ions from a very wide range of normally solid materials is described. Ion beams of high brightness at currents in the tens of microamps range can be readily generated and it is likely that, with further development, ion beams with far larger currents could be obtained.

The energy spread of the ions is very low, about 0.3 eV, a value very close to the thermal spread expected from a source at 2400^{0}K. Thus there is practically no spreading caused by other factors. The energy spreading is very much smaller than that commonly encountered in gaseous ion sources, typically several electron volts(ref.17), indicating that this source has advantages in applications requiring precise control of ion trajectories.

The purity of the beam is very high, being at least 99.9% pure provided the purity of the starting material is sufficiently high. This feature eliminates the need for mass separation of the beam in applications requiring pure ion beams. It is likely that the present main limitation to the beam purity, the presence of ions formed from residual gases, can be considerably reduced by fairly simple means.

Another desirable feature of the source is that it produces a negligible gas load on the vacuum system. Further, in many cases some gettering action by the material evaporated from the hot spot is likely, in which case the vacuum conditions may be improved by operating the source.

All these attributes make the source particularly suitable for many applications including ion implantation, micromachining, microprobe work, ion plating(ref.18) and perhaps even in isotope separation.

The only disadvantages associated with the source are its low ionization efficiency, about 0.07%, and the presence of multicharged and cluster species in the ion beam. The low ionization efficiency should only prove a problem in the case of expensive target materials, however such problems could be largely overcome by designing the source in such a way that condensed target material could be readily collected and reused.

10. ACKNOWLEDGEMENTS

I would like to thank Mr E.H. Hirsch for suggesting this investigation and for many useful discussions during the development of the source. My thanks also go to Mr B.A. Johnson and the late Mr S.A. Bricknell for help in constructing and assembling the source and associated equipment.

REFERENCES

No.	Author	Title
1	Richards, J.	"Ion Assisted Deposition of Tin Films". To be published
2	Krimmel, E.F.	Rev. Sci. Instr. 37, No.5, 678, (1966)
3	Krimmel, E.F.	Nucl. Instr. and Meth. 60, 231 (1968)
4	Krimmel, E.F.	Z. angew. Physik, 31, 51 (1971)
5	Kishi, T. and Nishidi, T.	Japan. J. Appl. Phys. 12, No.6, 954 (1973)
6	Kishi, T. and Sugata	Japan. J. Appl. Phys. 11, No.5, 773 (1972)
7	Beg, S. and Malik, N.A.	International J. of Mass Spect. and Ion Physics 27, 49 (1978)
8	Septier, A.	"Focussing of Charged Particles". Academic Press, N.Y., pp 131-156 (1967)
9	Lohmann, B. and Richards, J.	"A Parallel Plate Energy Analyser". ERL-0090-TR, 1979
10	Richards, J.	"A High Sensitivity Positive Ion Detector". ERL-0120-TM, 1980
11	van Steenbergen, A.	IEEE Trans. Nucl. Sci. NS-12, No.3, 746 (1965)
12	Daly, N.R.	Rev. Sci. Instr. 31, No.8, 264 (1960)
13	Schwarz, H.	J.A.P. 35, No.7, 2020 (1964)
14	Langmuir, I.	Phys. Rev., 2, 329 (1913)
15	Samsonov, G.V.	"Handbook of the Physiochemical Properties of the Elements". IFI/PLENUM, NY, p 255 (1968)
16	Von Engel, A.	"Ionized Gases". Clarendon Press, Oxford, p 63 (1965)
17	Von Ardenne, M.	"Tabellen zur angewandten Physik". Band 1, VEB Deutscher Verlag Der Wissenschaften, Berlin, pp 640-653, (1962)

No.	Author	Title
18	Mattox, D.M.	Electrochem. Technol., 2, 295 (1964)

TABLE 1. SUMMARY OF THE MASS SPECTRUM OF A TIN ION BEAM

Tin ions			Other ions		
Position on mass scale of commonest isotope	Likely species	Experimental yield (% of total)	Position on mass scale of commonest isotope	Likely species	Experimental yield (% of total)
120	Sn^+	64	208	Pb^+	0.66
60	Sn^{2+}	16	209	Bi^+	0.19
238	Sn_2^+	12.7	104	Pb^{2+}	0.12
356	Sn_3^+	3.3	18	$(H_2O)^+$	0.063
476	Sn_4^+	1.22	28	N_2^+	0.026
90	?	0.88	63	Cu^+	0.025
40	Sn^{3+}	0.21	32	O_2^+	0.020
594	Sn_5^+	0.20	104.5	Bi^{2+}	0.019
30	Sn^{4+}	0.10	17	$(OH)^+$	0.016
53.3	?	0.095	16	O^+	0.0032
37.5	?	0.051	14	N^+	0.0018
712	Sn_6^+	0.050	2	H_2^+	0.0016
45	?	0.021			
66.7	?	0.019			
24	Sn^{5+}	0.017			
150	?	0.015			
28.8	?	0.014			
33.6	?	0.005			
20	Sn^{6+}	0.004			

TABLE 2. SUMMARY OF THE MASS SPECTRUM OF A GERMANIUM ION BEAM

Germanium ions			Other ions		
Position on mass scale of commonest isotope	Likely species	Experimental yield (% of total)	Position on mass scale	Likely species	Experimental yield (% of total)
74	Ge^+	78.2	18	H_2O^+	0.01
146	Ge_2^+	15.7	28	N_2^+	0.01
37	Ge^{2+}	5.2	32	O_2^+	0.006
218	Ge_3^+	0.48			
55.5	?	0.16			
290	Ge_4^+	0.11			
24.67	Ge^{3+}	0.076			
364	Ge_5^+	0.05			

TABLE 3. POSSIBLE CHARGE EXCHANGE REACTIONS

Initial ion		Final ion			Initial ion		Final ion		
Species	Experimental yield (%)	Species	Expected position on mass scale	Experimental yield (%)	Species	Experimental yield (%)	Species	Expected position on mass scale	Experimental yield (%)
Sn^{2+}	16	Sn^{+}	240	*	Sn^{6+}	0.0035	Sn^{5+}	28.8	0.014
Sn^{3+}	0.21	Sn^{2+}	90	0.88	Sn^{6+}	0.0035	Sn^{4+}	45	0.021
Sn^{3+}	0.21	Sn^{+}	360	*	Sn^{6+}	0.0035	Sn^{3+}	80	
Sn^{4+}	0.10	Sn^{3+}	53.3	0.095	Sn^{6+}	0.0035	Sn^{2+}	180	
Sn^{4+}	0.10	Sn^{2+}	120	*	Sn^{7+}	-	Sn^{6+}	23.3	
Sn^{4+}	0.10	Sn^{+}	480	*	Sn^{7+}	-	Sn^{5+}	33.6	0.005
Sn^{5+}	0.017	Sn^{4+}	37.5	0.051	Sn^{7+}	-	Sn^{4+}	52.5	
Sn^{5+}	0.017	Sn^{3+}	66.7	0.019	Sn^{7+}	-	Sn^{3+}	93.3	
Sn^{5+}	0.017	Sn^{2+}	150	0.015					
Sn^{5+}	0.017	Sn^{+}	600	*	Ge^{3+}	0.076	Ge^{2+}	55.5	0.16

* Peaks are obscured by the presence of other tin species.

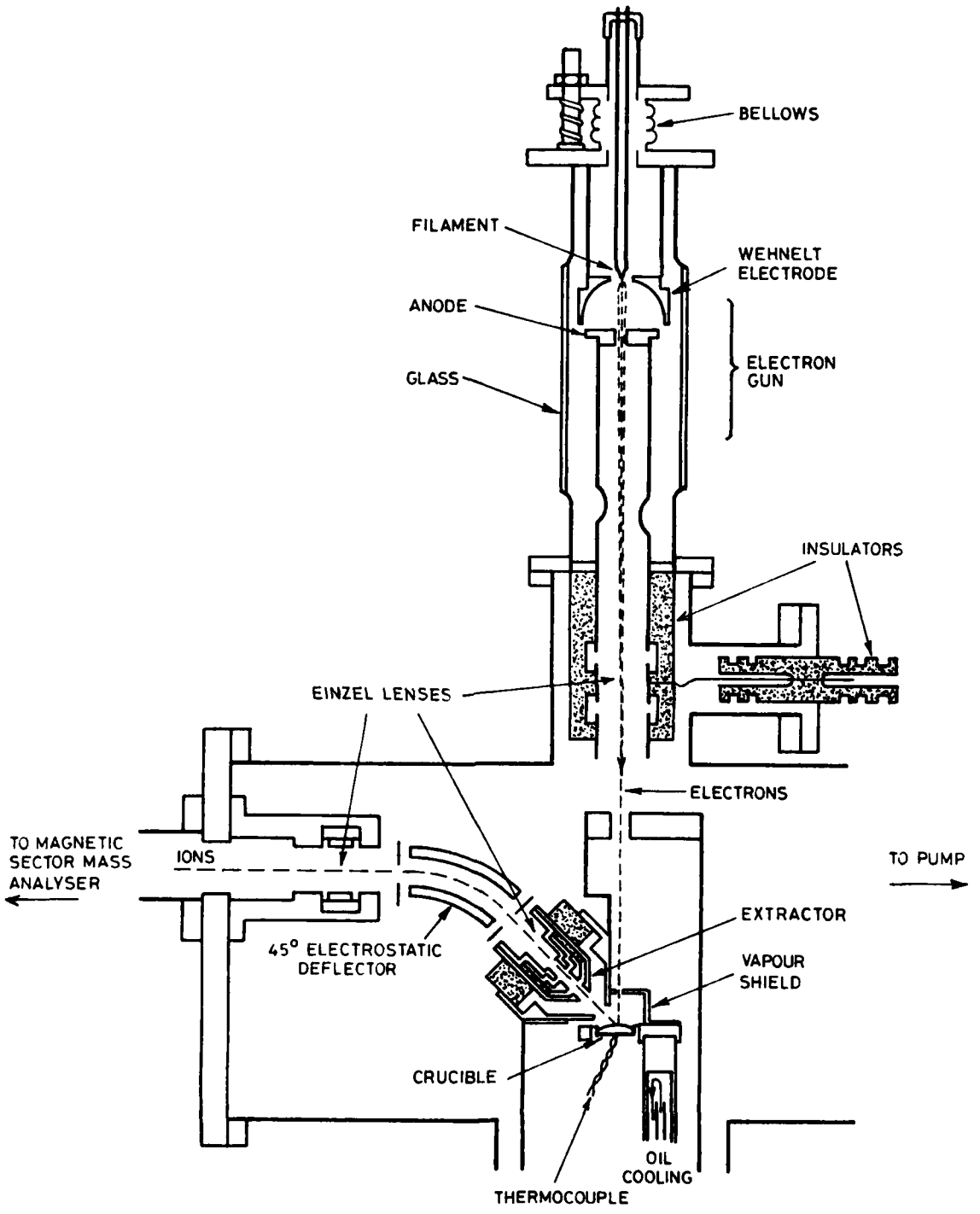

Figure 1. Diagram of ion source

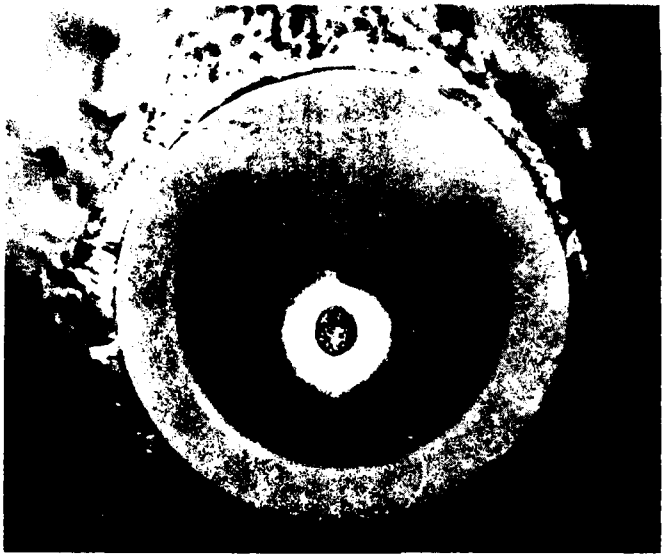

2.0 mm

Figure 2. Pattern formed on extractor electrode by tin ions and vapour using the extractor geometry shown in figure 1

0.1 mm

Figure 3. Enlargement of the region of the extractor at the centre of the ion beam

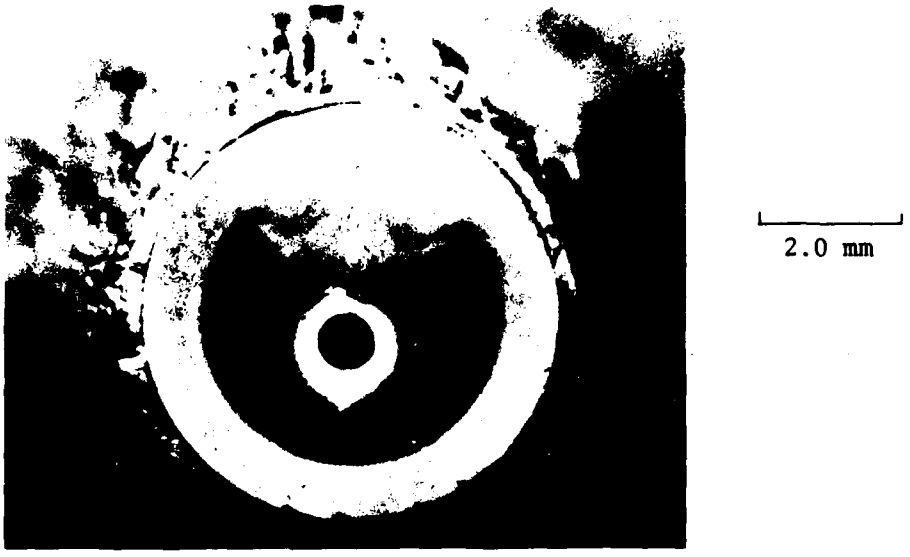

Figure 4(a). Extractor aperture used for examining the angular divergence of the ion beam

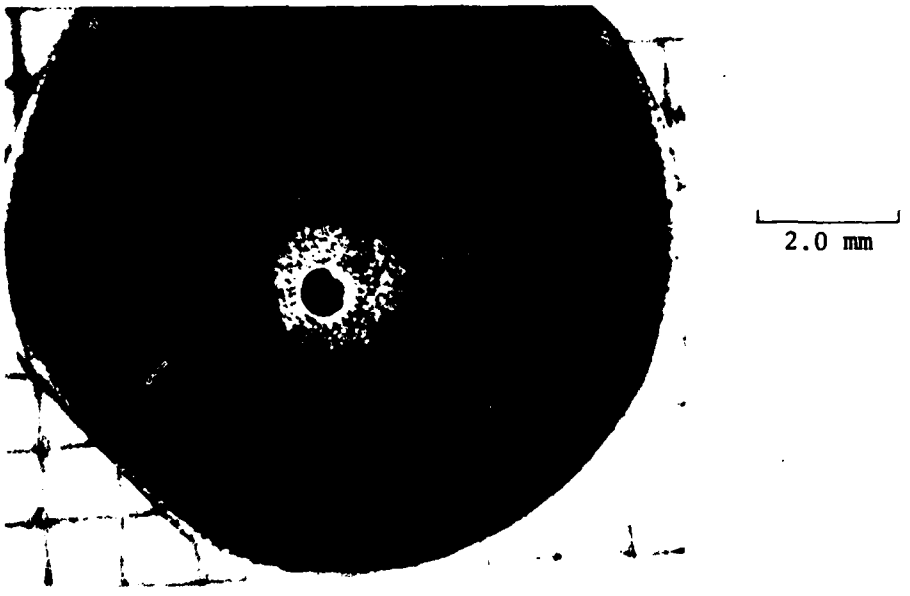

Figure 4(b). Pattern formed on copper disc placed 7 mm behind extractor

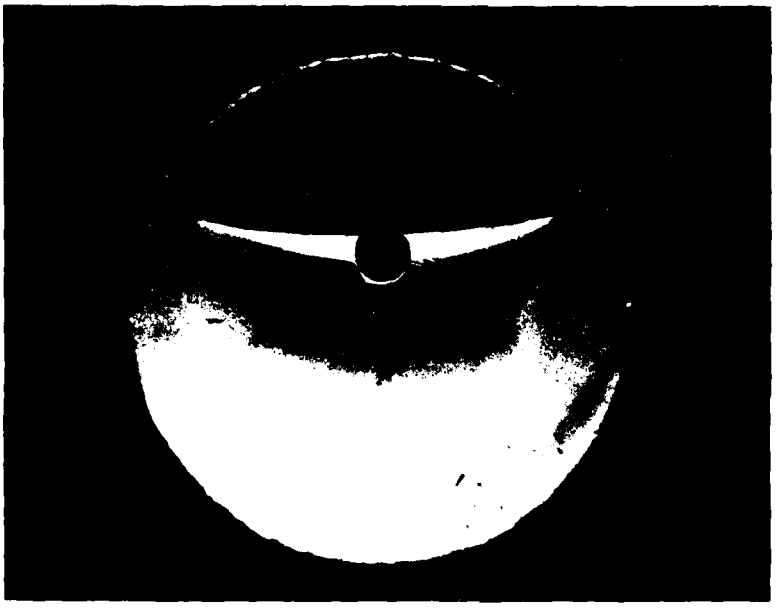

Figure 5(a). Pattern formed on extractor electrode by tin ions and vapour using an unshielded extractor

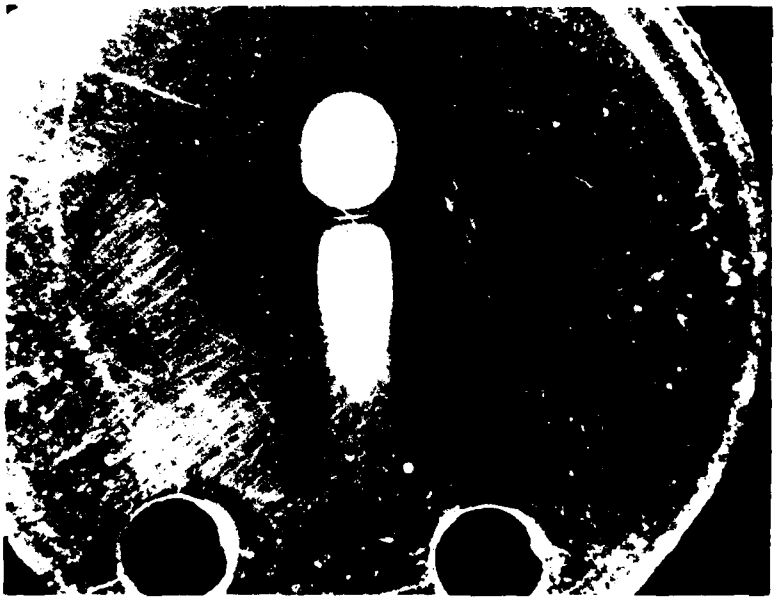

Figure 5(b). Pattern formed on copper disc placed 12 mm behind extractor

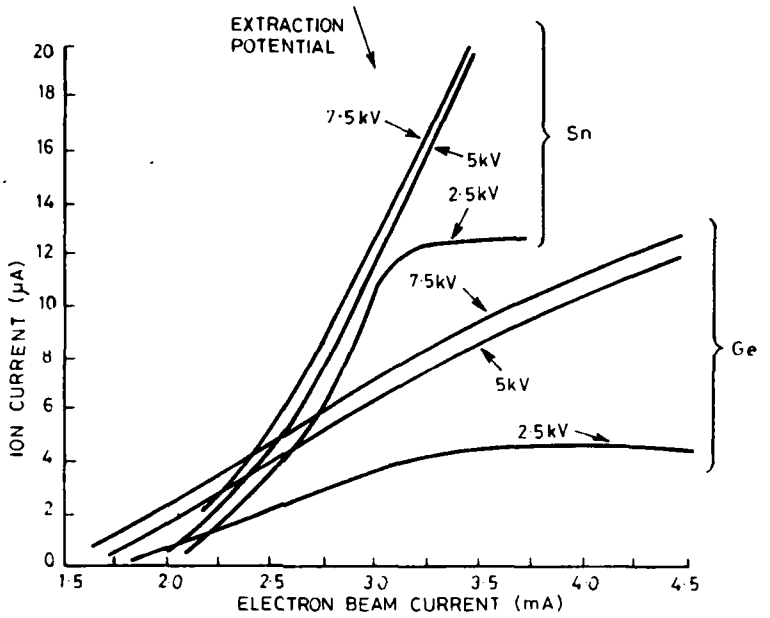

Figure 6. Dependence of ion current on electron beam current at various extraction potentials

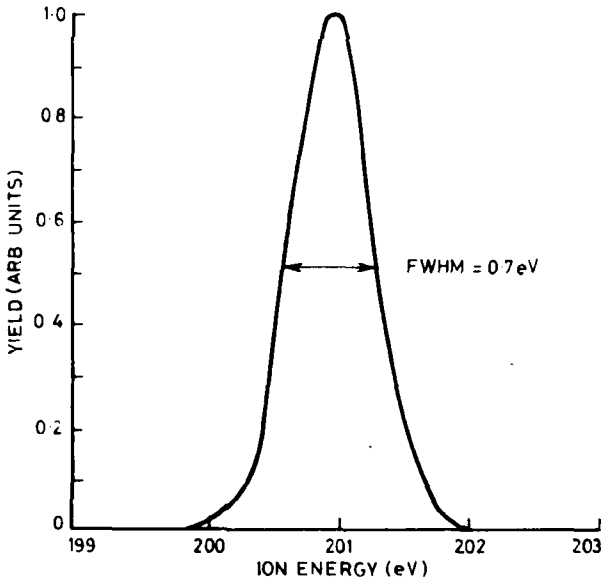

Figure 7. Energy distribution of tin ions

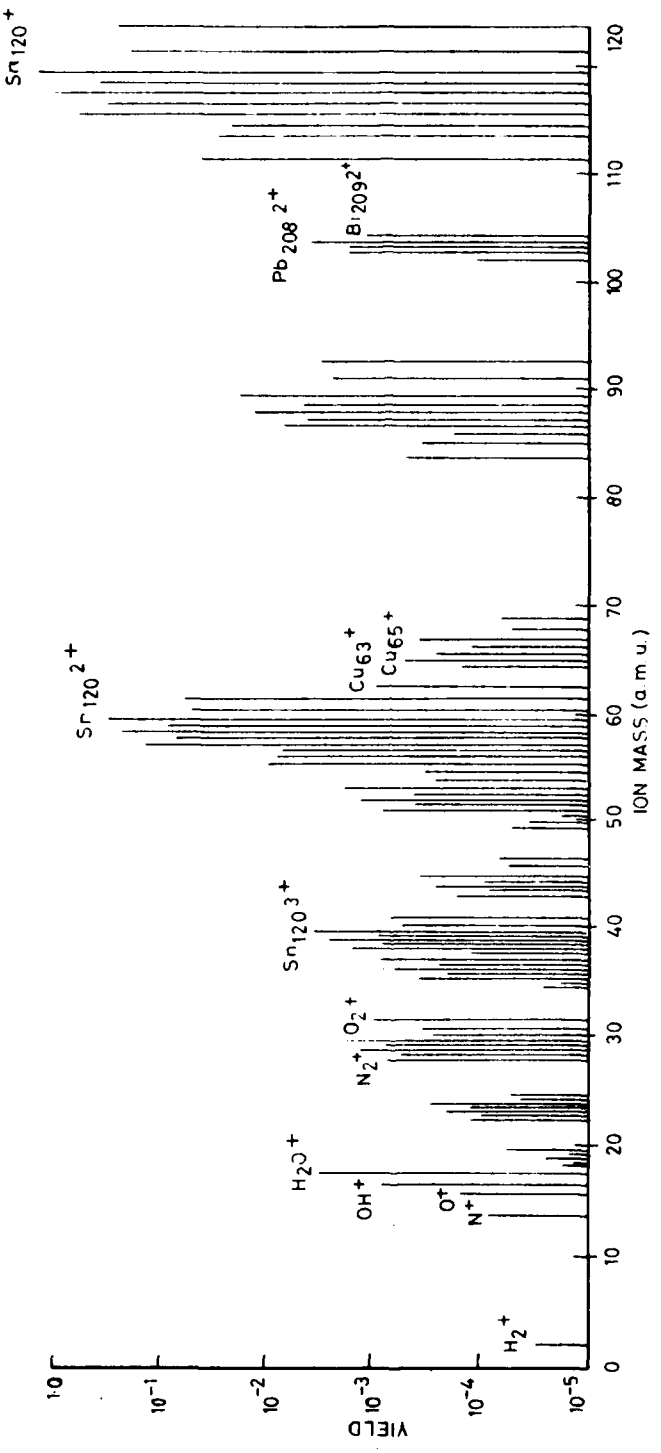

Figure 8. Mass spectrum of tin ion beam between 0 and 125 a.m.u.

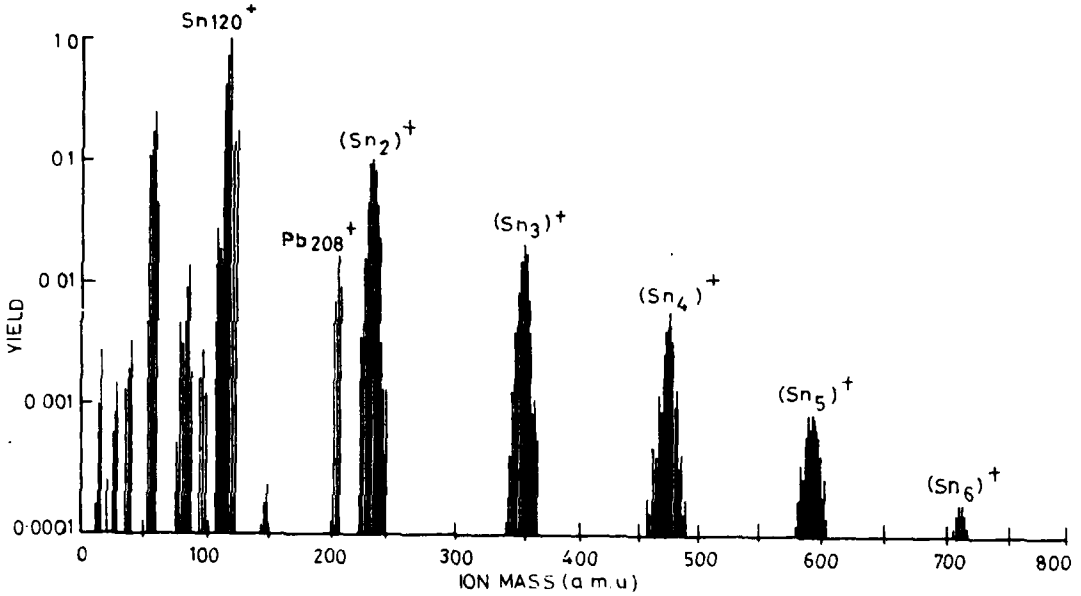

Figure 9. Mass spectrum of tin ion beam

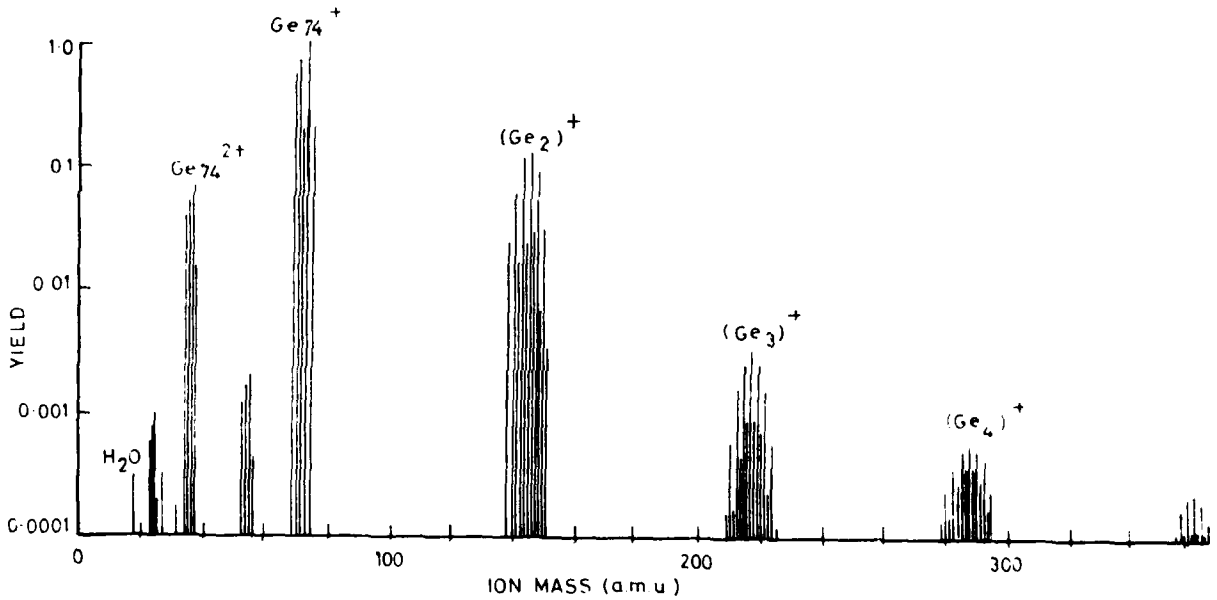

Figure 10. Mass spectrum of germanium ion beam

DISTRIBUTION

	Copy No.
EXTERNAL	
In United Kingdom	
Defence Scientific and Technical Representative, London	No copy
National Lending Library for Science and Technology Boston Spa, Yorkshire	1
Technology Reports Centre, Orpington, Kent	2
In United States of America	
Counsellor, Defence Science, Washington	No copy
National Technical Information Services Springfield, Va.	3
Engineering Societies Library, New York, NY	4
In Australia	
Chief Defence Scientist	5
Deputy Chief Defence Scientist	6
Controller, Projects and Analytical Studies	7
Superintendent, Major Projects	8
Superintendent, Science and Technology Programmes	9
Director, Joint Intelligence Organisation (DDSTI)	10
Defence Information Services Branch (for Microfilming)	11
Defence Information Services Branch for:	
United Kingdom, Ministry of Defence, Defence Research Information Centre(DRIC)	12
United States of America, Defence Technical Information Center	13 - 24
Canada, Department of National Defence, Defence Science Information Service	25
New Zealand, Ministry of Defence	26
Australia National Library	27
Defence Library, Campbell Park	28
Library, Aeronautical Research Laboratories	29
Library, Materials Research Laboratories	30

Document Exchange Commission for:

United Kingdom representative, Canberra	31
United States of America representative, Canberra	32
Canadian representative, Canberra	33
New Zealand representative, Canberra	34

WITHIN DRCS

Chief Superintendent, Electronic Research Laboratories	35
Superintendent, Navigation and Surveillance Division	36
Principal Officer, Laser Group	37
Mr E.H. Hirsch, Laser Group	38
Mr D. Rees, Laser Group	39
Mr N. Bromilow, Optical Techniques Group	40
Dr R.S. Seymour, Laser Group	41
Mr W.A.R. MacFarlane, Laser Group	42
Mr I.K. Varga, Laser Group	43
Author	44 - 48
DRCS Library	49 - 50
Spares	51 - 58

The official documents produced by the Laboratories of the Defence Research Centre Salisbury are issued in one of five categories: Reports, Technical Reports, Technical Memoranda, Manuals and Specifications. The purpose of the latter two categories is self-evident, with the other three categories being used for the following purposes:

Reports	:	documents prepared for managerial purposes.
Technical Reports	:	records of scientific and technical work of a permanent value intended for other scientists and technologists working in the field.
Technical Memoranda	:	intended primarily for disseminating information within the DSTO. They are usually tentative in nature and reflect the personal views of the author.